

EVOLUTION OF LATITUDE ZONAL STRUCTURE OF THE LARGE-SCALE MAGNETIC FIELD IN SOLAR CYCLES

V. I. MAKAROV

Kislovodsk Station of the Pulkovo Observatory, Kislovodsk, 357741, U.S.S.R.

and

K. R. SIVARAMAN

Indian Institute of Astrophysics, Bangalore 560034, India

(Received 25 January, 1985; in revised form 8 July, 1988)

Abstract. Properties of a latitude zonal component of the large-scale solar magnetic field are analyzed on the basis of $H\alpha$ charts for 1905–1982. Poleward migration of prominences is used to determine the time of reversal of the polar magnetic field for 1870–1905. It is shown that in each hemisphere the polar, middle latitude and equatorial zones of the predominant polarity of large-scale magnetic field can be detected by calculating the average latitude of prominence samples referred to one boundary of the large-scale magnetic field. The cases of a single and three-fold polar magnetic field reversal are investigated. It is shown that prominence samples referred to one boundary of the large-scale magnetic field do not have any regular equatorward drift. They manifest a poleward migration with a variable velocity up to 30 m s^{-1} depending on the phase of the cycle. The direction of migration is the same for both low-latitude and high-latitude zones. Two different time intervals of poleward migration are found. One lasts from the beginning of the cycle to the time of polar magnetic field reversal and the other lasts from the time of reversal to the time of minimum activity. The velocity of poleward migration of prominences during the first period is from 5 m s^{-1} to 30 m s^{-1} and the second period is devoid of regular latitude drift.

1. Introduction

The structure of the large-scale magnetic field on the Sun is determined by the distribution of unipolar regions which are evident on magnetograms. Alternatively the monopolar regions can be identified on $H\alpha$ synoptic charts (McIntosh, 1972, 1979). McIntosh developed guidelines for inferring magnetic polarities on the Sun from observations of filaments and filament channels. These charts, however, do not provide any information on magnetic field strengths. But when the features in the $H\alpha$ spectroheliograms can be identified clearly, the neutral line pattern of these large-scale magnetic fields can be derived with greater confidence and accuracy than can be inferred from magnetograms (Duvall *et al.*, 1977; Makarov, Stoyanova, and Sivaraman, 1982; Makarov and Stoyanova, 1982) especially in the regions of the weak fields and of the observations in polar zones. These $H\alpha$ charts represent ready material for investigating global properties of large-scale magnetic fields during many cycles of solar activity when $H\alpha$ observations have taken place but magnetographic observations are not available. These charts are more useful from the practical point of view as all boundaries of monopolar regions with length scales many times more than the dimensions of the supergranulation cells are available.

2. Construction of Synoptic Charts

McIntosh (1979) has constructed $H\alpha$ synoptic charts for the period 1964–1974. We prepared synoptic charts on the same line from the Kodaikanal $H\alpha$ and $Ca\ II\ K$ spectroheliograms for the solar rotations 675–1486 that correspond to the period 1904–1964. In addition to the filaments the prominences on the limb are sketched for every day on the same charts. The positions of the filaments were compared with the Meudon charts of filament distribution (C.S.C.S., 1919–1964). Prominences with optical depth less than one unity along the line-of-sight do not show up as filaments on the disc but only as filament channels, and even this does not occur on all occasions. Such prominences appearing day after day were noted from the spectroheliograms and from these the filament channels were mapped. When all these features (namely, filaments, filament channels, and prominences) were mapped on the Meudon charts, the continuous boundaries of the large-scale monopolar regions became quite obvious (Makarov, Stoyanova, and Sivaraman, 1982; Makarov, Fatianov, and Sivaraman 1983; Makarov, 1984a).

We have adopted McIntosh's (1979) rules for polarity inference, according to which the polarity signs (+ and –) are assigned on the basis of the polarity of the leading and following spots in the northern and southern hemispheres for any particular cycle. For the period 1870–1905 we had data from occasional prominence observations only (M.S.D.S.I., 1872–1911). We used the high-latitude structure of these phenomena, interpreting them as polar filament bands by analogy with $H\alpha$ charts. For the period 1964–1974 we used charts (McIntosh, 1979), *Solar Geophysical Data* (1973–1982), and *Solnechnye Dannye* Bulletin (1979–1982).

3. Treatment of Synoptic Charts

The synoptic charts show that the polarity of the large-scale magnetic field for any longitude alternates in sign at several latitudes between the equator and the poles, the line of demarcation being the filament bands that run approximately east to west. It is possible to assign a mean latitude to every filament band over each solar rotation. To make the value of the mean latitude quite representative we measure the latitudes of the filament band in every 20° longitude zone and average them over one solar rotation. This mean value forms one data point on the migration trajectory curve. By plotting all such points for the polemost filament as well as other filament bands as a function of time, we obtain the trajectory of the poleward boundaries of magnetic regions of one dominant polarity as they migrate to high latitude with the progress of solar activity.

4. On the Degree of Equivalence of the Average Location of the Neutral Lines and of the Large-Scale Magnetic Fields

$H\alpha$ synoptic charts are constructed from $H\alpha$ filtergrams or spectroheliograms which depict chromospheric features that are closely associated with photospheric magnetic

field structures. The association is so well established that the chromospheric features can be used as a good proxy for the magnetic structures (McIntosh, 1972; Duvall *et al.*, 1977; Topka *et al.*, 1982; Makarov, Stoyanova, and Sivaraman, 1982). The most important among the chromospheric features are $H\alpha$ filaments seen in the spectroheliograms that represent the neutral line of the radial component of the magnetic field on the Sun. Once, these neutral lines are identified and mapped unambiguously by accumulating information from spectroheliograms, the boundaries where polarity reverse becomes clear and so the distribution of the large scale magnetic field also becomes obvious.

A comparison of the average location of the neutral line with the pattern of the large scale magnetic field for cycles 20 and 21 (Howard and LaBonte, 1981; Makarov, Fatyanov, and Sivaraman, 1983) shows that the zonal boundaries from $H\alpha$ charts coincide sufficiently well with the polarity division line of the magnetic field. Also, the migration of the filament neutral lines agrees well with that of the large-scale magnetic fields seen in the diagram of Howard and LaBonte (1981).

5. The Latitude Zonal Structure of the Magnetic Field

$H\alpha$ synoptic charts contain data on evolution of the latitude and sector structure of large-scale solar magnetic fields. At the first stage we investigate the zonal structure only for understanding global properties such as latitude migration of the magnetic field, reversal of the Sun's polar magnetic field, etc.

The latitude zonal structure can be determined by:

(a) explaining the observed pattern of the magnetic field on spherical functions (Hoeksema, 1984; Stenflo and Vogel, 1986; Stenflo and Weisenborn, 1987; Stenflo, 1988);

(b) computing the mean latitude of the neutral magnetic lines (Makarov and Fatyanov, 1980; Makarov and Sivaraman, 1983; Makarov, 1984b);

(c) computing the magnetic field flux of the dominant polarity in separate narrow latitude zones;

(d) computing the latitude distribution of the magnetic field polarity at the same longitudes from rotation to rotation during a given cycle (Makarov and Kushmir, 1986), etc.

Each of these methods has its own advantages and disadvantages. We have determined the zonal structure by the *b*-method, i.e., by mapping boundaries of the latitude zones in order to clearly see the evolution of the zonal structure from cycle to cycle. Although we have lost sight of some details but the main ones were distinguished since it is known that the mean latitudes of the filament bands are in good agreement with the neutral line locations as received from the magnetic data (Topka *et al.*, 1982).

6. Results

The general evolutionary pattern of mean latitudes of global magnetic neutral lines on the Sun during activity cycles is shown in Figure 1. The zonal structure of the magnetic

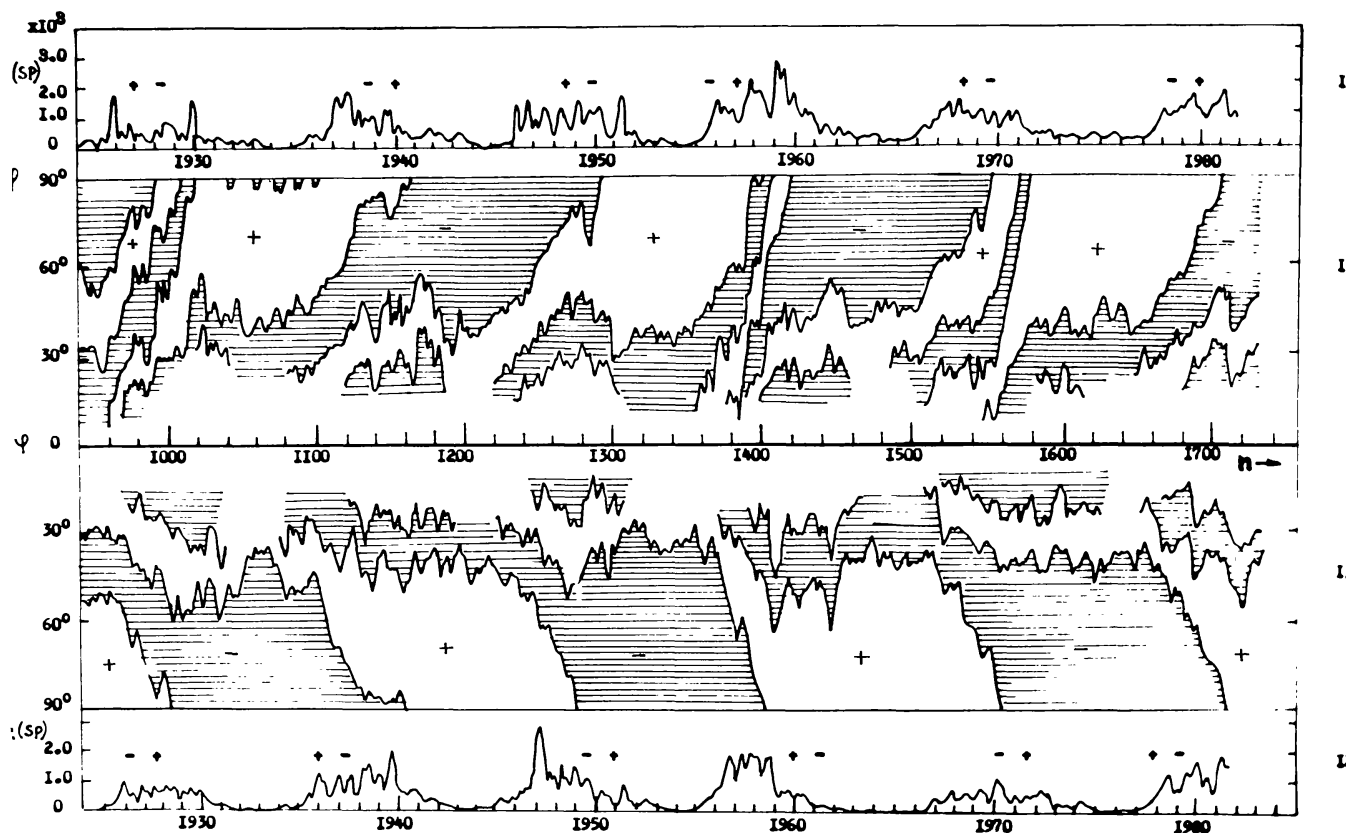


Fig. 1a. Curves in boxes II and III are migration trajectories of the mean latitude (averaged over three rotations) of the large scale magnetic field neutral lines in solar cycles 16–21 (northern and southern hemispheres). ‘+’ and ‘-’ stand for the magnetic field polarity signs in the conventional way. The start of a new boundary corresponds to that on $H\alpha$ chart where the total length of the polarity division line along the longitude exceeds 240° . n is the number of the Carrington solar rotation. Time is in years. Curves in boxes I and IV are plots of daily sunspot areas averaged over three rotations (northern and southern hemisphere, respectively). $A(S_p)$ are expressed in 10^{-6} of the visible hemisphere. These areas are extracted from the Greenwich photographic results published before 1976, 1977–1982 data are given from the *Solnechnye Dannye Bulletin*.

field and its evolution is well defined. For example, we compared part of Figure 1 for the 20th solar cycle (Carrington rotations 1540–1585) with the magnetic data in Figure 2 (reproduction of Figure 4 in Topka *et al.*, 1982). The comparison of our data with those by Howard and LaBonte (1981) and Topka *et al.* (1982) shows that the mean latitude of zone boundaries and their evolution coincide with the polarity division lines of the large scale magnetic field in a solar cycle. So, the method of $H\alpha$ charts enables us to analyse the behaviour of low l -modes of the large scale field and to watch the process of reversal of the Sun’s polar magnetic field. As is seen from Figure 1 large-scale magnetic field cycles can be divided into 3 types according to the number of latitude zones which reach the poles:

1st type: a single reversal of the polar magnetic field is observed in both hemispheres. This phenomenon took place in solar cycles Nos. 11, 13, 15, 17, 18, 21.

2nd type: a 3-fold reversal of the polar magnetic field is observed in one of the

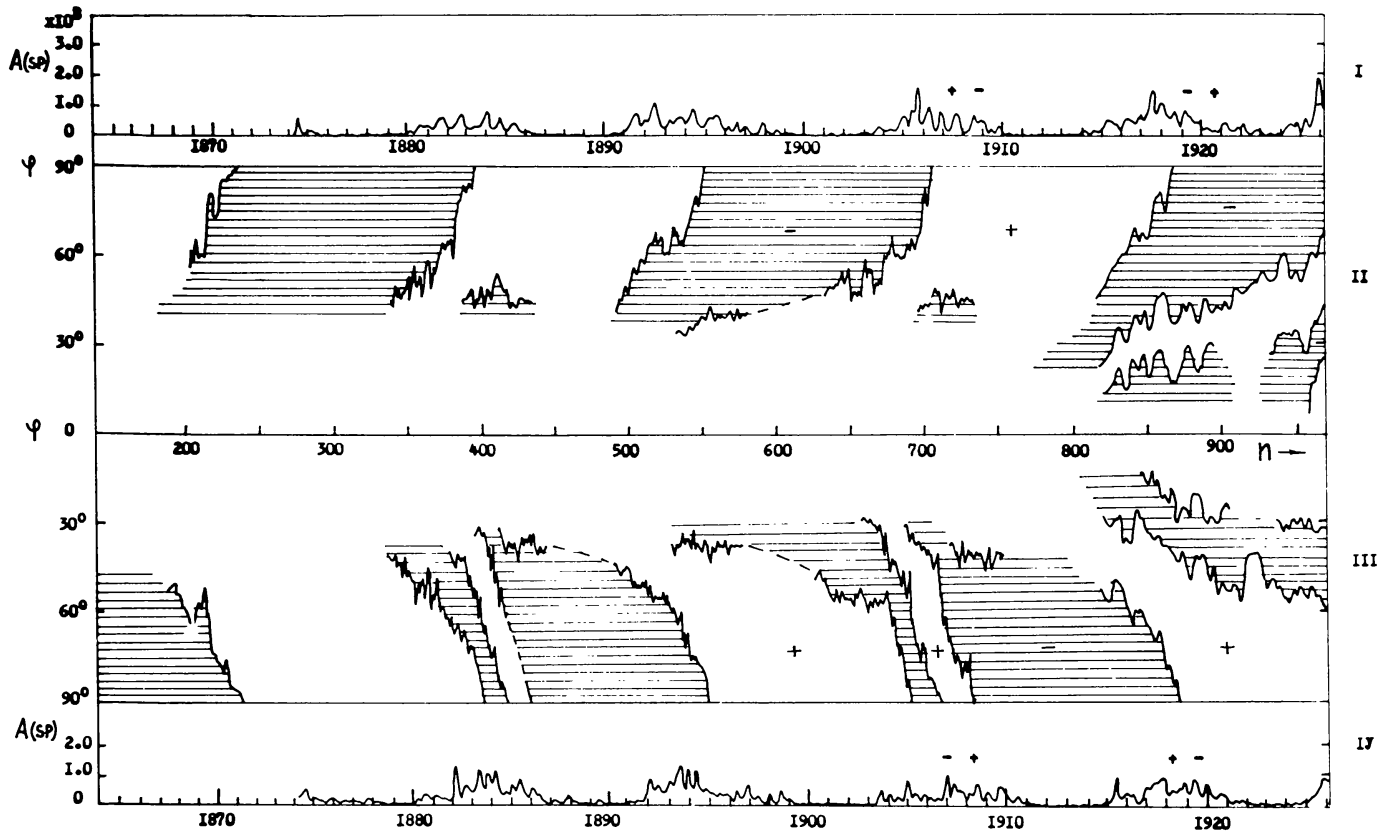


Fig. 1b. The trajectories of migration of the mean latitude of prominences during 1870–1905 were plotted using prominence observations in Italy (M.S.D.S.I.).

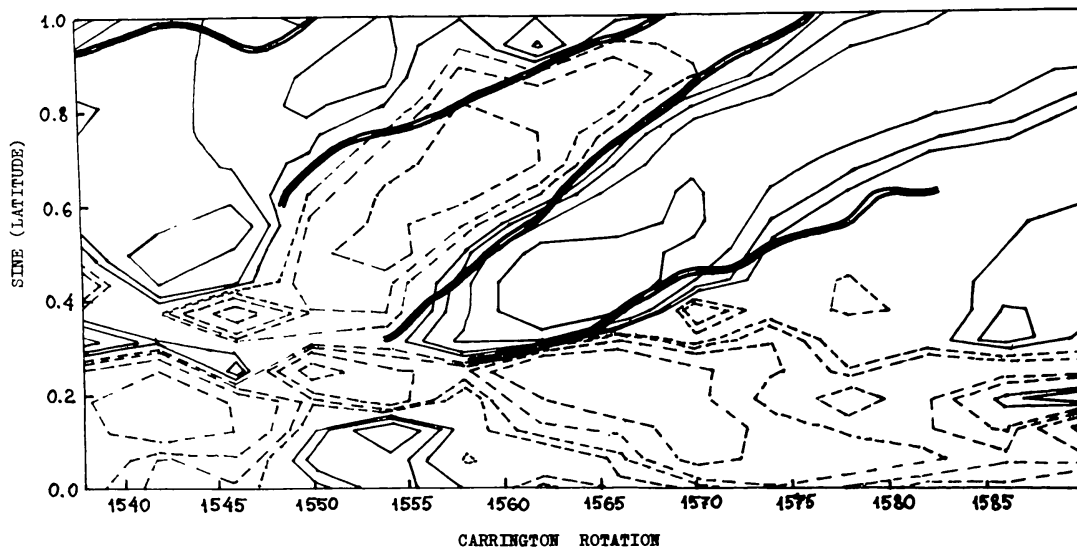


Fig. 2. The mean latitude of the large-scale magnetic field neutral lines in the Carrington rotations 1540–1585 as a function of time (same as Figure 1), superimposed upon the average magnetic field according to Howard and LaBonte (1981). (Reproduction of Figure 4 in Topka *et al.*, 1982).

hemispheres, whereas only a single reversal is observed in the other. This took place in solar cycles Nos. 12, 14, 16, 19, 20.

3rd type: a three-fold reversal of the polar field takes place in both hemispheres. This phenomenon has not been observed during the last 115 years.

As is seen from Figure 1 the number of polar magnetic field reversals in a solar cycle is associated with the evolution of the zonal structure. Hence, let us analyse the 1st and 2nd types of solar cycles separately.

6.1. SINGLE FIELD REVERSAL CYCLES

Before the 1981 reversal, as can be seen in Figure 1, the southern hemisphere high-latitude zone of the negative magnetic field had migrated from the equatorial latitudes. It had originated in the middle of solar cycle 19 in 1956–1958. This was located at the middle latitudes before the beginning of solar cycle 20, 1965–1966, and it determined the sign of the magnetic field of the polar zone during 1970–1980. A similar pattern of latitude zone evolution in the southern hemisphere was observed in all the cycles from 15 to 21 (1910–1982) when single reversals were observed. One can see that the time of latitude zone evolution in this case is about 22 years.

Using solar cycles 19 (1955–1964) as an example, it has been shown (Makarov, 1983) that formation of new magnetic field zones and peculiarities in their poleward drift are due to activity bursts. New field zones were formed during the cycle against the background of the fields of the 'old' equatorial zone from the preceding cycle. The epoch of formation of the zones in each hemisphere coincides in time with enhanced emergence of new active regions and quasicircular filaments (Makarov and Tavastsherna, 1983). The polar migration velocity of latitude zone boundaries does not exceed 10 m s^{-1} in the case of a single polar field reversal. The above peculiarities in magnetic field behaviour, as derived from $H\alpha$ charts, are confirmed by magnetographic observations during 1958–1982 (Babcock, 1959; Howard and LaBonte, 1981; Makarov, 1983).

6.2. THREE-FOLD FIELD REVERSAL CYCLES

Figure 1 shows that a three-fold reversal took place in solar cycles 16, 19, and 20 in the northern hemisphere and in solar cycles 12 and 14 in the southern hemisphere. Magnetographic observations confirm this phenomenon in solar cycles 19 and 20 (Howard and LaBonte, 1981; Makarov, 1983).

From Figure 1 (northern hemisphere) it can be seen that all three magnetic field latitude zones observed after the reversal of the polar magnetic field in solar cycle 18 (about 1950) reached the N-pole in the 19th solar cycle (1958–1960). This zonal latitude migration caused three-fold reversals of the polar field. The reversals lasted for 3 years from 1958 to 1960. After the field reversal in 1960, three new zones of the large-scale magnetic field emerged during solar cycle 19. They then reached the pole and caused a three-fold polar field reversal during solar cycle 20 in 1969–1971. The formation of new latitude zones was also caused by bursts of activity (Makarov and Tavastsherna, 1983). In those cycles with a three-fold reversal, all three zones migrated poleward with a velocity of about 30 m s^{-1} , which is three times as fast as those in single reversal

cycles. As can be seen from Figure 1, the zonal evolution time in the case of a repeated three-fold reversal is about 10–12 years.

6.3. POLEWARD MIGRATION OF LATITUDE ZONE BOUNDARIES

In accordance with classical methods, two zones of filament evolutions are observed. One of them is a low-latitude zone (from 0° to $\pm 40^\circ$) that is connected with sunspots. It repeats the Maunder diagram with respect to the number of filaments. The second zone is a high latitude one in which filament activity is observed only during the first half of the cycle. The filaments of the second zone definitely migrate poleward. We determined the filament coordinates and the latitude migration of filaments in dependence on their lifetime for the low-latitude zones $\varphi \leq 30^\circ$ and high latitude zones $\varphi > 30^\circ$ from Meudon Synoptic Charts for solar cycle 18 and 19 (1944–1965). It has been shown that filaments manifest a poleward migration at all the latitudes (Bortsov and Makarov, 1987). This concept of filament poleward migration at all latitudes was considered earlier (d’Azambuja and d’Azambuja, 1944; Makarov and Fatianov, 1980; Topka *et al.*, 1982; Makarov, 1984c).

It follows from Figure 1 that there is no regular equatorward migration of latitude zone boundaries at any phase of the cycle. During several solar rotations one can trace an equatorward shift of the zone boundaries, but subsequently they tend to return to their initial locations. Only regular poleward migration of zone boundaries or quasi-periodic variations of their latitudes relative to their mean position are observed (Makarov *et al.*, 1985). However, poleward migration of the zone boundaries with a velocity from 5 to 30 m s^{-1} is observed only in the first half of the cycle, i.e., from the beginning of the cycle to the epoch of polar field reversal. After the epoch of reversal the poleward migration of the zone boundaries ceases drastically and stays at this level until minimum activity. At this time the latitude of the zone boundaries oscillates quasi-periodically with velocities from 3 to 5 m s^{-1} , amplitude from 3 to 5 heliographic degrees and a period of about 18 solar rotations (Makarov *et al.*, 1985a). The nature of such oscillations has not yet been discovered as there is no data on the variations of the latitude of separate filaments in time more than 1.5 years. It seems that the zone boundary oscillations can be connected with the emergence of new monopolar regions of the large scale magnetic field and averaging of the neutral line positions.

6.4. IS POLEWARD MIGRATION OF LATITUDE ZONE BOUNDARIES SOLAR-CYCLE RELATED?

Using Mount Wilson magnetograph data, Howard and LaBonte (1981) show that the polar fields are entirely formed by the movement of magnetic field from the sunspot latitudes to the poles. This formation is not continuous but episodic and the apparent velocity of poleward motion of magnetic fields is not constant during the spot cycle.

On the other hand, enough evidence has now been accrued both from direct line-of-sight velocity measurements as well as indirect measures using tracer elements like $\text{H}\alpha$ filaments to establish the existence of a poleward flow on the Sun with a velocity from 42 to 20 m s^{-1} over a 10° – 50° latitude band (Beckers, 1977; Duvall, 1979; Howard, 1979).

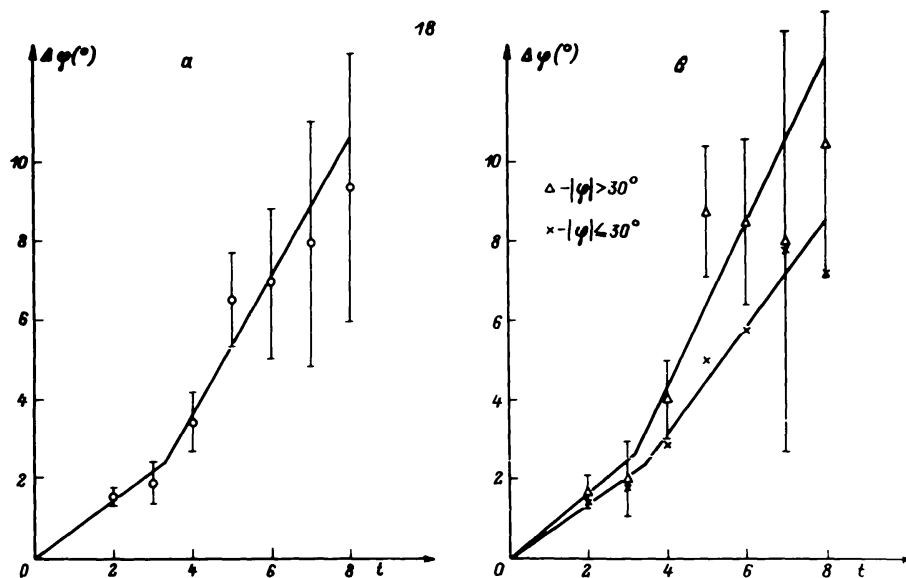


Fig. 3a. The latitude difference $\Delta\varphi$ of a single H α filament as a function of age according to C.S.C.S. for solar cycle 18. t in Carrington rotation, positive $\Delta\varphi$ note poleward migration, according to Bortsov and Makarov (1987).

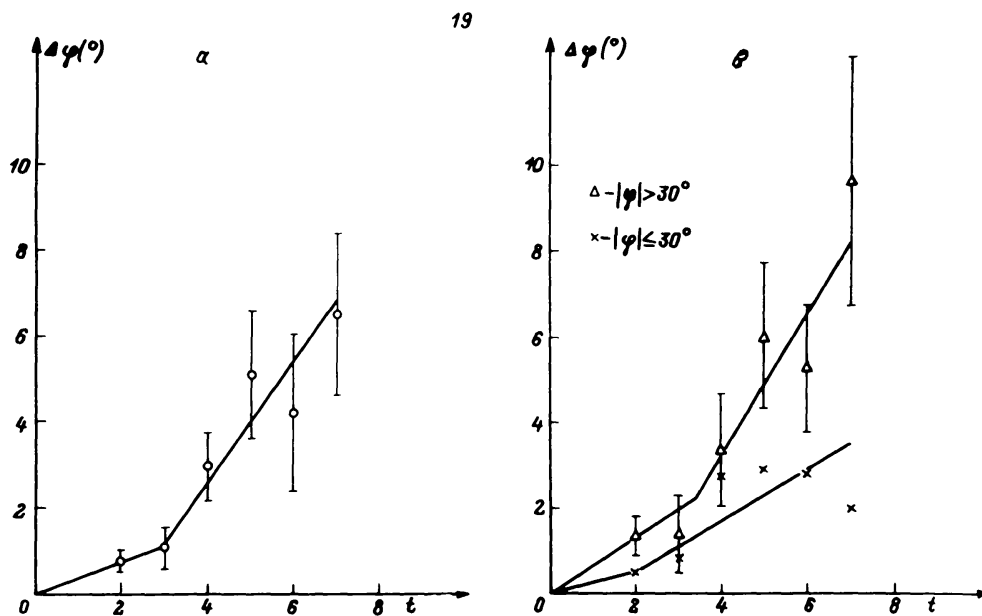


Fig. 3b. Same as Figure 3(a) for solar cycle 19.

Alternatively, the filaments seen in the H α spectroheliograms are essentially magnetic lines and can be used as effective and reliable tracers for measuring poleward motion (Topka *et al.*, 1982; Makarov and Sivaraman, 1983). They represent migration of large-scale regions from equatorial latitudes towards the poles. In Figure 1 we can see clearly that the zone boundaries have poleward migration with a velocity from 10 to

30 m s^{-1} , during the rising phase of the cycle to the time of the polar magnetic field reversal. Then the regular polar drift of the zone boundaries ceased. An analysis of H α filament migration for 1904–1982 established clearly that poleward migration starts at the beginning of the solar cycle with drift velocities of about $3\text{--}5 \text{ m s}^{-1}$. As the cycle progresses the drift velocity peaks at 30 m s^{-1} . At the cycle maximum one or three filament bands reach the poles reversing the poloidal field polarity. A comparison of our data with those of Howard and LaBonte (1981) for the period 1967–1980 shows that the global properties of magnetic field latitude migration coincide. The nature of such variations of the poleward migration of the zone boundaries has not yet been discovered. According to Howard and LaBonte (1981) this change may be either a real variation in the velocity of the flow transported by the field or artifact of the differing polarity variation of polar and moving fields.

Acknowledgements

One of us (M.V.I.) is grateful to Dr R. A. McCutcheon, of Computer Sciences Corporation, for improving the quality of the English language translation of the paper.

References

- Babcock, H. D.: 1959, *Astrophys. J.* **130**, 364.
 Beckers, J. M.: 1977, in G. Belvedere and L. Paterni (eds.), *Workshop on Solar Rotation*, Univ. of Catania, p. 166.
 Bortsov, V. V. and Makarov, V. I.: 1987, *Soln. Dann.* No. 11.
 C.S.C.S. – *Cartes Synoptiques de la Chromosphere Solaire*: 1919–1964, Rotations No. 877–1486, Meudon, France.
 d’Azambuja, L. and d’Azambuja, M.: 1944, *Ciel Terre* **60**, Nos. 7–8–9, 6.
 Duvall, T. L.: 1979, *Solar Phys.* **63**, 3.
 Duvall, T. L., Wilcox, J. M., Svalgaard, L., Scherrer, P., and McIntosh, P. S.: 1977, *Solar Phys.* **55**, 63.
 Hoeksema, J. T.: 1984, *C.S.S.A.-Astro-84-07*, p. 1.
 Howard, R.: 1979, *Astrophys. J.* **228**, L45.
 Howard, R. and LaBonte, B. J.: 1981, *Solar Phys.* **74**, 131.
 Makarov, V. I.: 1983, *Soln. Dann.* No. 10, 93.
 Makarov, V. I.: 1984a, *Soln. Dann.* No. 6, 59.
 Makarov, V. I.: 1984b, *Soln. Dann.* No. 9, 52.
 Makarov, V. I.: 1984c, *Solar Phys.* **93**, 393.
 Makarov, V. I. and Fatianov, M. P.: 1980, *Soln. Dann.* No. 10, 96.
 Makarov, V. I. and Kushnir, M. V.: 1986, *Soln. Dann.* No. 4, 63.
 Makarov, V. I. and Sivaraman, K. R.: 1983, *Solar Phys.* **85**, 227.
 Makarov, V. I. and Stoyanova, M. N.: 1982, *Soln. Dann.* No. 11, 94.
 Makarov, V. I. and Tavastsherna, K. S.: 1983, *Soln. Dann.* No. 5, 93.
 Makarov, V. I., Stoyanova, M. N., and Sivaraman, K. R.: 1982, *Astrophys. Astron. J.* **3**, 379.
 Makarov, V. I., Fatianov, M. P., and Sivaraman, K. R.: 1983, *Solar Phys.* **85**, 215.
 Makarov, V. I., Tavastsherna, K. S., and Petrova, N. N.: 1985, *Soln. Dann.* No. 6, 69.
 McIntosh, P. S.: 1972, *Rev. Geophys. Space Phys.* **10**, 837.
 McIntosh, P. S.: 1979, ‘Annotated Atlas of H-alpha Synoptic Charts’, World Data Center A for Solar Terrestrial Physics, NOAA, Boulder, Colorado.
M.S.D.S.I.–Memorie d. Soc. d. Spetr. Ital., 1872–1911; 1–40.
Solar Geophysical Data: 1973–1982, Nos. 348–436.
Soln. Dann.: 1979–1982, Nos. 1–12.

- Stenflo, J. O.: 1988, *Astrophys. Space Sci.* (in press).
- Stenflo, J. O. and Vogel, M.: 1986, *Nature* **319**, 285.
- Stenflo, J. O. and Weisenborn, A. L.: 1987, *Solar Phys.* **108**, 205.
- Topka, K., Moore, R., LaBonte, B. J., and Howard, R.: 1982, *Solar Phys.* **79**, 231.